Archives of Mechanics • Archiwum Mechaniki Stosowanej • 30, 4–5, pp. 629–643, Warszawa 1978

Two-dimensional calculations of an explosion in the real atmosphere

L. V. SHURSHALOV (MOSCOW)

TWO-DIMENSIONAL or axisymmetrical non-stationary gas flow which arises when a cylindrical or a spherical charge explodes in the real non-homogeneous atmosphere is studied. The explosions are modelled by the expansion of the corresponding volumes containing compressed hot gas. The finite-difference Godunov's method with some necessary modifications is applied to the solution of the arising gasdynamical problem. Non-isothermal properties of the real undisturbed atmosphere and thermodynamical high-temperature characteristics of air are taken into account. The comparison with the analogous results obtained for the isothermal (exponential) atmosphere and the perfect gas is carried out. On the basis of the two-dimensional numerical solution the accuracy of the well-known approximate modified Sachs scaling rule, which allows to determine shock wave intensity in a non-homogeneous atmosphere using the corresponding data for a homogeneous atmosphere, is evaluated. Significance of the results obtained for the determination of the Tunguska meteorite trajectory and energetic parameters is discussed.

Badany jest dwuwymiarowy lub osiowo-symetryczny przepływ gazu wywołany wybuchem cylindrycznego lub sferycznego ładunku w rzeczywistej niejednorodnej atmosferze. Wybuchy modelowane są ekspansją odpowiednich objętości zawierających podgrzany gaz. Do rozwiązania wyżej omówionego zagadnienia gazodynamicznego zastosowano metodę różnic skończonych Godunowa z pewnymi niezbędnymi modyfikacjami. Uwzględniono nieizotermiczne własności rzeczywistej niezaburzonej atmosfery i termodynamiczne wysokotemperaturowe charakterystyki powietrza. Przeprowadzono porównania rozwiązania z wynikami analogicznymi otrzymanymi dla izotermicznej (wykładniczej) atmosfery i gazu doskonałego. Na podstawie dwuwymiarowego rozwiązania numerycznego wyznaczono dokładność dobrze znanego przybliżonego, zmodyfikowanego prawa podobieństwa Sachsa, które pozwala określić intensywność fali uderzeniowej w niejednorodnej atmosferze, wykorzystując odpowiednie dane dla atmosfery jednorodnej. Przedyskutowano znaczenie otrzymanych wyników dla określenia trajektorii i parametrów energetycznych meteorytu Tunguskiego.

Исследуется двумерное или осесимметричное течение газа, вызванное взрывом цилиндрического или сферического заряда в реальной неоднородной атмосфере. Взрывы моделируются расширением соответствующих объемов, содержащих подогретый газ. Для решения вышеобсужденной газодинамической задачи применен метод конечных разностей Годунова с некоторыми необходимыми модификациями. Учтены неизотермические свойства реальной невозмущенной атмосферы и термодинамические высокотемпературные характеристики воздуха. Проведено сравнение решения с аналогичными результатами, полученными для изотермической (экспоненциальной) атмосферы и идеального газа. На основе двумерного численного решения определена точность хорошо известного приближенного модифицированного закона подобия Сокса, который позволяет определить интенсивность ударной волны в неоднородной атмосфере, используя соответствующие данные для однородной атмосферы. Обсуждено значение полученных результатов для определения траекторных и энергетических параметров Тунгусского метеорита.

1. Introduction

DURING the last ten years considerable attention has been paid in the theory of explosion to the study of two-dimensional effects caused by the non-homogeneity of the real Earth's atmosphere. In particular, the "strong" stage of an explosion, i.e. when counter-pressure

of the shock in front can be neglected, was investigated in detail [1–4]. For many applications, including those from meteoritics, consideration of the late stage of an explosion in a non-homogeneous atmosphere, when the shock wave goes far from the source and the counter-pressure cannot be neglected, is of prime importance. For the perfect gas model and an isothermal exponential atmosphere such a two-dimensional solution taking into account gravity force was numerically obtained by the author [5] on the basis of the Godunov finite-difference method [6, 7]. The present paper generalizes the previous results to the case of the non-isothermal standard atmosphere and high-temperature properties of real air. The explosion energies and heights considered are chosen close to those which might have taken place at the gigantic Tunguska explosion in 1908. Gasdynamical aspects of the Tunguska meteorite problem were studied lately by V. P. KOROBEINIKOV, P. I. CHUSHKIN and L. V. SHURSHALOV [8–13].

2. Gasdynamical models

Undisturbed pressure p and density ϱ in the non-homogeneous Earth's atmosphere are supposed to be dependent only on the vertical coordinate z which is counted off further on from sea level. Two models of the atmosphere are considered. In the simplest isothermal exponential atmosphere

$$p = p_* \exp(-z/z_*), \quad \varrho = \varrho_* \exp(-z/z_*), \quad g = p_*/(\varrho_* z_*). \tag{2.1}$$

Here z_* is the scale height of the atmosphere, p_* and ϱ_* are the pressure and the density at $z = 0$, g is the acceleration of gravity. The real Earth's atmosphere is not isothermal. Its average, so-called standard conditions are tabulated. Convenient analytic fits were built up [13], representing the table data to within 0.5% in the height range from 0 to 60 km. Their general form is as follows:

$$f = a + b\xi + c\xi^2 + d\xi^3, \quad \xi = (z - z_0)/(z_1 - z_0) \tag{2.2}$$

The values of $\log p$, $\log \varrho$ and g are taken as f. The coefficients in Eqs. (2.2) for g in the whole considered height range are $a = 9.8066$, $b = -0.1845$, $c = 0.0026$, $d = 0$, with g in m/sec^2. The height interval $0 \div 60$ km was divided into three parts for p and ϱ: $z_0 \leqslant z \leqslant z_1$ ($z_0 = 0$ km, $z_1 = 10$ km; $z_0 = 10$ km, $z_1 = 30$ km; $z_0 = 30$ km; $z_1 = 60$ km). The corresponding coefficients for these three intervals are shown in Table 1.

Here the pressure p is expressed in kg/m^2, while the density ϱ is in kg sec^2/m^4.

For the numerical procedure it does not matter which atmosphere model is considered. But results may differ rather essentially, what will be illustrated in the following.

Two kinds of explosions in the non-homogeneous atmosphere are considered: one of a spherical charge and the other of a cylindrical charge inclined under the angle α to the Earth's surface. In the latter case the plane sections' hypothesis (which has evident limitations, of course) is used. On account of it the three-dimensional problem is reduced to a two-dimensional one: the consideration of a flow in a plane perpendicular to the charge's axis. In all cases an explosion is modelled by an expansion of compressed hot gas volumes. It is simple, on one hand, and it provides better representation of some significant

Table 1.

$\log p$ kg/m²	$0 \leqslant z \leqslant 10$ km	$10 \leqslant z \leqslant 30$ km	$30 \leqslant z \leqslant 60$ km
a	4.0142	3.4316	2.0817
b	−0.5156	−1.3496	−1.9532
c	−0.0543	−0.0508	0.5295
d	−0.0127	0.0505	−0.2672
$\log \varrho$ kg sec²/m⁴	$0 \leqslant z \leqslant 10$ km	$10 \leqslant z \leqslant 30$ km	$30 \leqslant z \leqslant 60$ km
a	−0.9034	−1.3750	−2.7386
b	−0.4175	−1.3057	−2.0934
c	−0.0436	−0.0465	0.4541
d	−0.0105	−0.0115	−0.0929

features of an explosion of finite volume charges, on the other. The plane sections, hypothesis in the cylindrical explosion case suggests that some effective values of the acceleration of gravity $\bar{g} = g \cos\alpha$ and atmosphere scale height $\bar{z}_* = z_*/\cos\alpha$ for the isothermal atmosphere or the corresponding alteration of the length scales for the standard atmosphere should be introduced. The general qualitative features of spherical and cylindrical explosions appear quite similar. That is why the computational results for a spherical explosion will mainly be discussed later on.

In our calculations air is considered as a non-viscous non-heat-conducting gas whose caloric equation of state is in the form

$$\varepsilon(p, \varrho) = p/[\varrho(\gamma-1)]$$

in which p is the pressure, ϱ the density, ε the internal energy per unit of mass. Both, a perfect gas having the constant value of the adiabatic index $\gamma = \gamma_0 = 1.4$ and a real gas with $\gamma = \gamma(p, \varrho)$ are considered. Table data of the air thermodynamic characteristics within the wide range of temperatures from very low up to millions of degrees Kelvin exist (see, for example, [14]). There are also different analytic fits to the table data. We use BRODE'S analytic form [15] which represents the thermal and caloric properties of air to within 10% in the density and temperature range of interest. In the cases considered the temperatures T are high enough to take into account various dissociations and ionizations of molecules and atoms in high-temperature air and, at the same time, not so high in order that radiative processes strongly affect the explosion dynamics ($200°\mathrm{K} < T < 30.000°\mathrm{K}$). Use of an effective adiabatic index $\gamma(p, \varrho)$ leads in the method [6, 7] to some complication of the calculation procedure and the corresponding increase of the computing time.

With the understanding of what has been said, the equations of motion governing the flow from an explosion in a non-homogeneous atmosphere will have the form

$$\varrho\, du/dt + \partial p/\partial r = 0, \quad \varrho\, dw/dt + \partial p/\partial z = -\varrho g,$$

$$d\varrho/dt + \varrho(\partial w/\partial z + \partial u/\partial r + \nu u/r) = 0,$$

$$\partial E/\partial t + \partial[w(E+p)]/\partial z + \partial[u(E+p)]/\partial r + \nu u(E+p)/r = -\varrho g w,$$

$$E = \varrho[\varepsilon + (u^2+w^2)/2].$$

Here u and w are the velocity components along the radial r and vertical z coordinates, correspondingly, $\nu = 0.1$ for a cylindrical and a spherical explosions, accordingly.

The g terms in the equations are very important. One can neglect them only while considering the early "strong" stage of an explosion, as it is ordinarily done [4]. The consideration of all explosion stages up to the "weak" one does not allow such a neglect because it leads to a catastrophic deterioration of results.

3. Numerical aspects

The blast calculations were carried out by the finite-difference GODUNOV's method [6, 7] with some modifications specific for the problem under consideration. A good choice of the network is important. Here it is built up in the polar coordinates R, θ with the origin at the explosion centre. Firstly, we use a moving computational grid in which the shock wave is treated as its boundary line with all the necessary boundary conditions being exactly satisfied. The shock front distinguishing technique considerably improves the accuracy of the solution as a whole. Secondly, the radial size of network cells is taken to be variable according to some law so that it diminishes while approaching the shock front and is automatically handled to the flow. This provides a better representation of hydrodynamic functions in the zone of their maximum gradients. Thirdly, uniform approximation along the angular coordinate θ is required. The network angle division is formed by uniformly distributed rays $\theta = \text{const.}$ beginning at the central point of the explosion. Fourthly, from the same considerations the difference scheme is built up in a somewhat non-standard way. In it the basic divergent form of continuity and energy equations is chosen ordinarily [7], while for two momentum equations it is taken as it was proposed for all equations in the work [16]. The purpose is that the two-dimensional difference scheme should give the best possible results if one solve is the one-dimensional problem, as well, i.e. that the results along different angle directions should not differ at all or differ minimally. Fifthly, the convergence of the grid rays $\theta = \text{const.}$ at a single point accounts for a computational singularity. Cells which are neighbouring geometrically do not turn out to be neighbouring computationally. Because of this effect disturbances come to some central cells from others, adjacent to them, with a time delay and this deteriorates the quality of the solution. To exclude that the central triangle cells are united in one, a polygon (or two polygons: upper and lower). In addition, this procedure increases the difference scheme stability and correspondingly decreases the computational time, all the more that just within that central region maximum temperatures and sound speeds take place.

While calculating explosions in the atmosphere one should keep in mind that sooner or later the shock will reach the Earth's surface and the problem of a reflection calculation then arises. This problem is in itself a rather complicated one and, generally speaking, demands special attention. In our calculations reflection processes are taken into account within one and the same difference scheme and network. In this case, then, details of reflection in the vicinity of the shock wave-Earth's surface intersection point are lost, they only contribute to the integral picture of the process. Consequently, one has to introduce here a non-standard five-cornered cell. In the region near the ground surface far from the intersection point the accuracy achieved is of the same order as for the solution as a whole.

4. Results

Some results of an explosion calculation in the real non-homogeneous atmosphere are discussed in the following. In the examples presented initial blast parameters are taken close to those that may be interesting for the investigation of the Tunguska meteorite problem studied in detail in the works [8–13].

To begin with we consider an explosion of energy $E_0 = 10^{23}$ erg occurring at a height $H = 8$ km above sea level. The explosion is not a point-source blast but an expansion of a finite spherical volume containing a compressed hot gas. Initial data within the volume are chosen so that the shock wave quickly approaches the point-source blast regime; in other words a low hot gas density within the spherical volume is taken. The influence of different factors on shock wave strength is clearly seen in Fig. 1. Here the shock overpres-

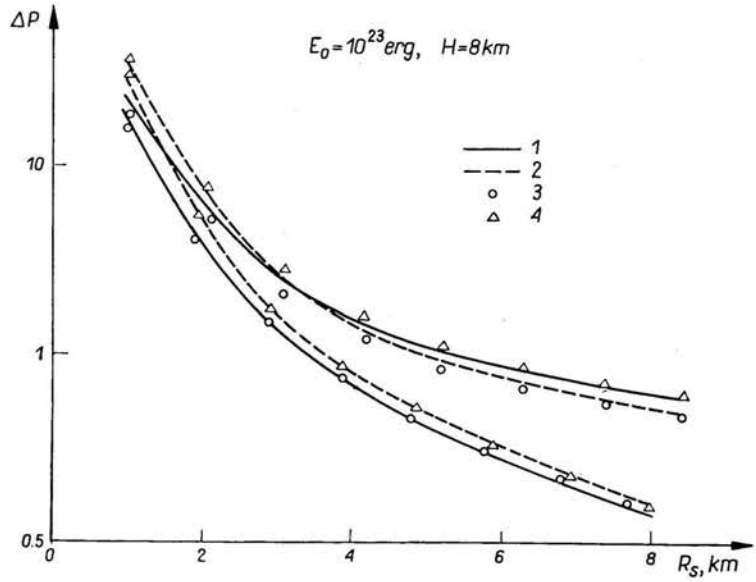

FIG. 1. Peak overpressure $\Delta P = (p_s - p_1)/p_1$ versus shock radius R_s for the upper and lower parts of the shock. 1 — real gas, standard atmosphere, 2 — perfect gas, exponential atmosphere, 3 — real gas, exponential atmosphere, 4 — perfect gas, standard atmosphere.

sure $\Delta P = (p_s - p_1)/p_1$ (p_s is the shock pressure, p_1 is the ambient atmosphere pressure immediately outside the shock) is depicted as a function of the shock radius R_s. The set of the lower/upper curves corresponds to the blast wave part propagating vertically down/upwards. The solid lines show the results for the real non-isothermal atmosphere and real gas, the air physical-chemical high-temperature properties being considered. The dashed curves give analogous data for the isothermal exponential atmosphere and perfect gas with $\gamma_0 = 1.4$. Circles and triangles indicate intermediate cases: 1) the isothermal atmosphere and real air, 2) the standard atmosphere and perfect gas, correspondingly.

Though Fig. 1 represents results for one set of initial parameters, the mutual position of the curves is the same for the broad range of energies E_0 and moderate heights H ($H \leqslant$

$\leqslant$ 10 km) and also for a cylindrical explosion. Therefore, Fig. 1 may serve as an illustration of the role of the non-isothermal atmosphere properties and high-temperature characteristics of real air. First of all, it is seen that results for the lowering part of the shock (the lower set of data) for real air inthe exponential and standard atmospheres are very close out at considerable distances. The same is true for the perfect gas model. Hence, it follows that the lowering front parameters out at far radii from the source do not depend substantially on which of the two mentioned atmosphere models is used. This conclusion is especially important for the Tunguska meteorite problem for which just parameters of the lowering shock wave are of interest. Thus these parameters can be determined with good accuracy by means of the isothermal atmosphere model.

One should keep in mind only the following. The isothermal (exponential) atmosphere may be chosen differently. The constants p_*, ϱ_*, z_* in the relations (2.1) may be taken from the conditions at sea level, at the blast point or at any other point of the atmosphere. Then, strictly speaking, the exponential and standard atmospheres coincide only in this single point and nowhere more. In general, the greater the distance from this point, the more they differ. In our calculations those constants are chosen from the standard sea level air conditions, what provides proximity of the two atmosphere models near the Earth's surface. Consequently, shock wave intensities near the ground happen to be close.

For the raising part of the shock, as it is seen from Fig. 1, the results for the isothermal and standard atmospheres considerably differ. This is accounted for by the marked difference in these two atmosphere models at high altitudes. In the height range between 0 and 17 km, which is characteristic for this example, the standard atmosphere pressure is everywhere lower than in the exponential atmosphere, the standard atmosphere density is lower between 0 and 12 km, then it is higher than in the exponential atmosphere.

Figure 1 shows that shock wave intensity in real air is lower than in perfect gas. The difference is 75–100% at the beginning, then it decreases down to approximately 10%. It is clearly seen that for the lowering shock it is more important to incorporate in the calculation the real air properties than the non-isothermal distributions of the atmosphere. Hence, by solving the inverse Tunguska meteorite problem with due consideration of high-temperature effects in air, one may get somewhat altered Tunguska explosion energy estimations obtained for the present by means of the perfect gas model [10, 12].

For an approximate determination of shock wave parameters in a non-homogeneous atmosphere, the well-known modified Sachs scaling rule exists. It postulates that for an explosion in a non-homogeneous atmosphere the shock wave strength at a point where $p = p_1$, $\varrho = \varrho_1$ is the same as the shock wave intensity at the same distance R from the source for an identical explosion in a homogeneous atmosphere whose constant ambient pressure and density are p_1 and ϱ_1. M. LUTZKY and D. L. LEHTO [17] compared the Sachs rule with the quasi-one-dimensional blast calculations in an exponential atmosphere for the case of the lowering shock waves. It turned out that the Sachs rule gave shock waves intensities to within 20% lower than the quasi-one-dimensional solution. It is interesting to find out what is the relation of the Sachs rule with respect to the two-dimensional numerical solution for all parts (lowering and rising) of the shock wave and for both spherical and cylindrical explosions.

Figure 2 shows the dependences $\Delta P(R_s) = (p_s - p_1)/p_1$ calculated for a spherical ($E_0 = 10^{23}$ erg, $H = 8$ km, solid lines) and a cylindrical ($E_0 = 1.4 \cdot 10^{17}$ erg/cm, $H = 13$ km, $\alpha = 40°$, dashed curves) blasts in an exponential atmosphere by means of the two-dimen-

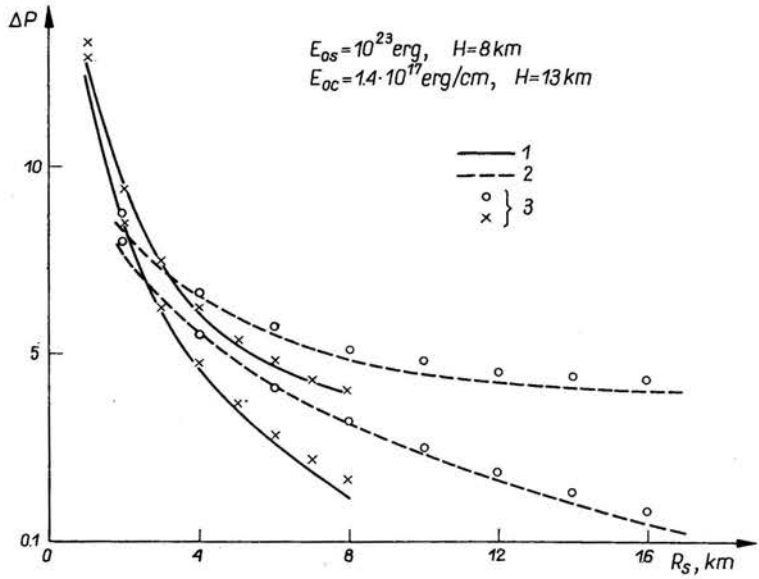

FIG. 2. Comparison between the two-dimensional solution and the modified Sach's rule for spherical and cylindrical explosions.
1 — spherical explosion, 2 — cylindrical exlosion, 3 — modified Sach's rule.

sional numerical procedure and the corresponding results obtained with the help of the Sachs rule (crosses for a spherical, circles for a cylindrical explosion). The upper/lower curves conform to the vertically rising/lowering shock front part. As it is seen, the Sachs rule gives quite good results not only for the lowering but also for the raising part of the shock. For the lowering shock the maximum difference between the Sachs and two-dimensional values of ΔP lies within 15—20 %, the Sachs rule giving higher intensities here. For other values of energies and altitudes this relation between the Sachs rule and the two-dimensional solution is approximately kept. Therefore, the simple Sachs rule gives better results than the quasi-one-dimensional numerical solution, at least for the lowering shock waves. Unfortunately, there are no data in [17] concerning rising blast waves but apparently the situation will be the same for them, too. Anyway, the use of the simple Sachs rule while performing the Tunguska explosion calculations, as it was done in [8–12], is fully justified. It leads only to a comparatively low (up. to 20%) raising of shock wave intensities and a corresponding understating of the explosion energy estimations in the solution of the inverse problem.

The way the explosion energy is distributed in space in a non-homogeneous atmosphere is a significant question, especially from the point of view of applicabilities of various quasi-one-dimensional techniques. The first calculations of a "strong blast" in a non-homogeneous atmosphere [1] demonstrated that there was a flow of energy upwards.

However, until recently, a detailed picture of this process at all stages of explosion has not been ascertained. Only in [5, 13] the question was elucidated for the case of an isothermal atmosphere and perfect gas model.

Before speaking about the explosion energy distribution it is interesting and useful to trace out the way the flow is changed with time. The flow (velocity) fields for an explosion with $E_0 = 6.5 \cdot 10^{22}$ erg and $H = 6.5$ km at two instants $t = 5.4$ sec and $t = 19$ sec are shown in Figs. 3 a, b. Because of the large difference in shock radii at these two mo-

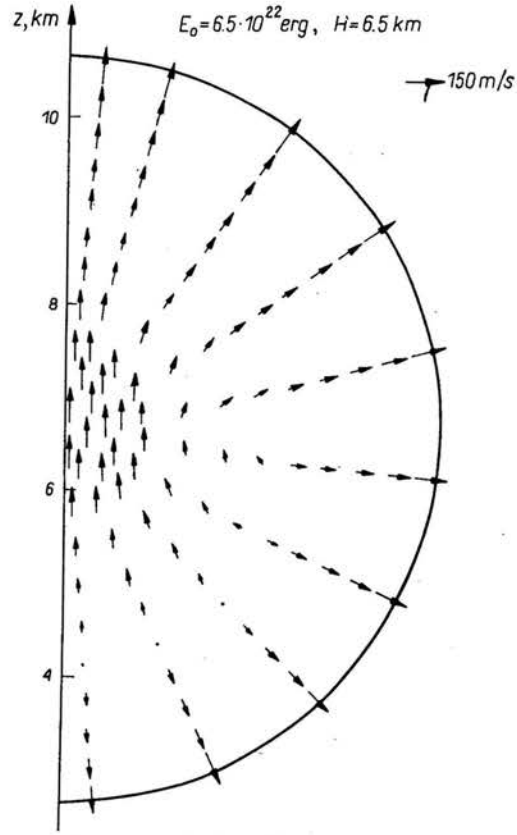

FIG. 3a. Velocity field at $t = 5 \cdot 4$ sec.

ments, a different length and velocity scales (indicated in the figures) are used here. At the instant $t = 19$ sec the shock wave has already reached the ground ($z = 0$) and reflection from the surface is calculated. As it is seen, initial radial velocity distribution which is characteristic for the one-dimensional flow is changed at first (Fig. 3a) in such a way that a powerful gas flow upwards arises in the central part of the disturbed region. Then, at later times (Fig. 3b), the flow is whirled and a ring-shaped vortex is formed. The latter effect is typical for explosions in a non-homogeneous atmosphere. Its origin lies in the end in the action of gravity. Thus, as one may note, at later times the flow acquires a rather complicated character.

The exchange of energy between the lower and upper parts of the disturbed region as a function of time t for a spherical explosion with $E_0 = 10^{23}$ erg and $H = 8$ km is shown in Fig. 4. An integral of the form

$$E = \iiint_{\Omega} \left[\frac{p}{\gamma - 1} - \frac{p_1}{\gamma_0 - 1} + \varrho \frac{V^2}{2} + (\varrho - \varrho_1) gz \right] d\Omega \tag{4.1}$$

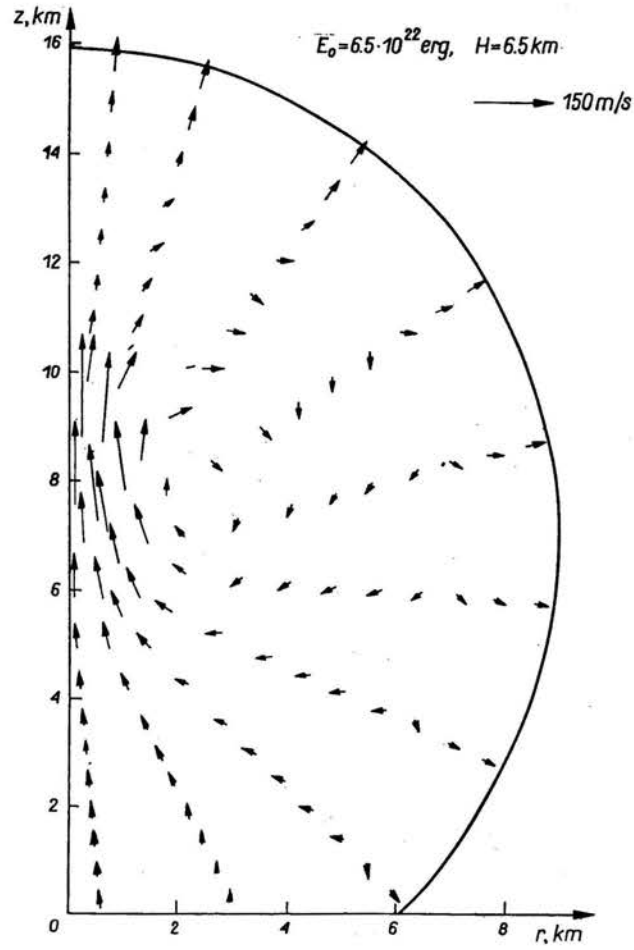

FIG. 3b. Velocity field at $t = 19$ sec.

over the upper and lower halves of the calculation region is computed here, the value obtained being divided by E_0. The results for the real air and standard atmosphere are drawn by the solid lines, for the perfect gas and exponential atmosphere by the dashed curves, for the real air and exponential atmosphere by circles, for the perfect gas and standard atmosphere by triangles. The dash-dotted straight line corresponds to the case of a homogeneous atmosphere when energy exchange between the bottom and top does not occur.

As it is seen, the difference between these four cases is not considerable. Nevertheless, one may note that the atmosphere type is less substantial for the energy partition than the gas model. Data for standard and isothermal atmospheres are practically the same, while for real air and perfect gas they somewhat differ. At the beginning the upward energy flows is a little bit more intensive for real air, at later times the same is true for perfect gas. On the whole, the energy division between the lower and upper parts of the disturbed region proceeds very actively and grows with time.

A more detailed picture of energy redistribution for the same blast is depicted in Fig. 5. Here, for each solid angle Ω_θ integrals of the form (4.1) are computed and are then divided

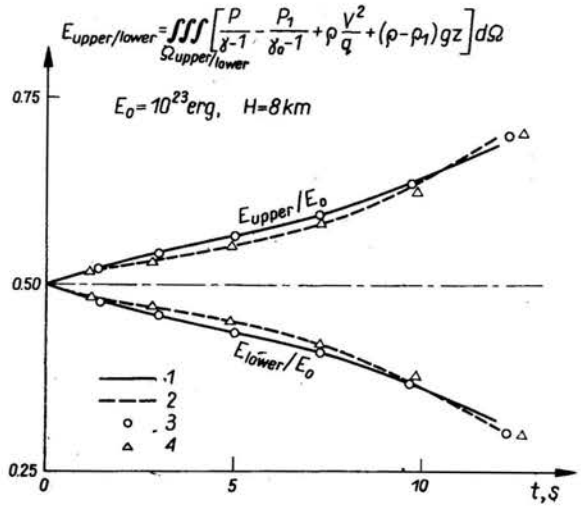

FIG. 4. Energy partition between the lower and upper parts of the disturbed region.
1 — real gas, standard atmosphere, 2 — perfect gas, exponential atmosphere, 3 — real gas, exponential atmosphere, 4 — perfect gas, standard atmosphere.

by the initial value of energy $E_0(\theta)$ in the same solid angle. In the one-dimensional case, when no energy flow in angular directions exists, the mentioned ratio is equal to a unit (the dash-dotted straight line). It rapidly changes in the two-dimensional case. The four different models are considered here, as in Fig. 4, and designations are left the same. The energy distributions and effects caused by the chosen models are more complicated here. First of all, beginning from some moment and for all the models, the dependence $E(\theta)/E_0(\theta)$ stops to be monotonic in the vicinity of $\theta = \pi/2$ (θ is counted off from the vertical in the upward direction). That means that locally not only the energy flow upwards takes place but also a small quantity of energy flows in the opposite direction. This is connected with the above-mentioned complex character that the flow acquires at later times. While comparing results for different models one should keep in mind that distributions in Fig. 5 correspond to the same radii R_s covered by the shock in the $\theta = \pi/2$ direction but to different instants t because shock intensities in the models differ noticeably and these equal the distances the shock waves traverse for different time intervals. For example, the dashed curve almost everywhere corresponds to a smaller energy exchange. Apart from other considerations this is so because the corresponding times for this model are the least.

The real gas model results in the standard and isothermal atmospheres are appreciably different. The difference grows in magnitude with time t and is especially pronounced at $\theta < 45°$ and $\theta > 135°$. As the general feature of all the models one may still remark that, beginning from some t, in the vicinity of $\theta = 0°$ the function $E(\theta)/E_0(\theta)$ becomes negative. That means that from such a zone more energy has flowed out than there was in the undisturbed atmosphere.

Figure 6a, b is a plot of the reduced pressure p/p_* and density ϱ/ϱ_* distributions at indicated times along the vertical $r = 0$ for a spherical explosion with $E_0 = 10^{23}$ erg and

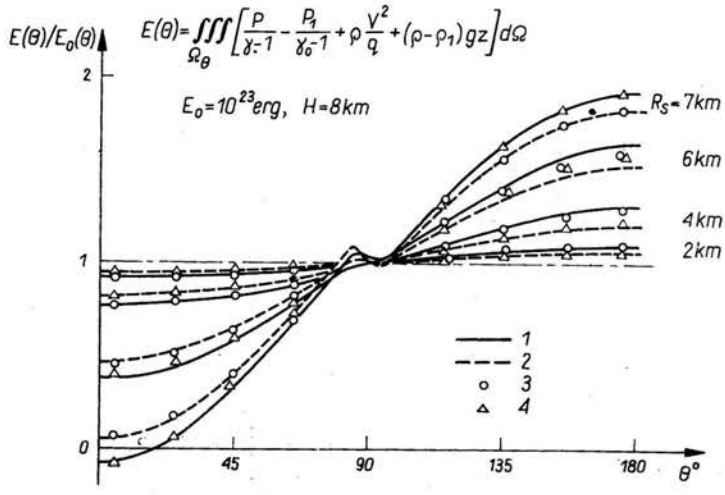

FIG. 5. Energy distribution as a function of a polar angle θ.
1 — real gas, standard atmosphere, 2 — perfect gas, exponential atmosphere, 3 — real gas, exponential atmosphere, 4 — perfect gas, standard atmosphere.

$H = 8$ km. The solid curves show the results for the real air, standard atmosphere model. Analogous data for the perfect gas, isothermal atmosphere model are marked by crosses. The undisturbed pressure and density dependences on the z coordinate are indicated by the dashed curves. Though maximum temperatures in this example take place in the central region, where the main difference between the real and perfect gas models may naturally be expected, it turns out that the most pronounced difference in the results is observed near the shock front. As it is better seen for the pressure at the shock, it is much lower in real air, especially in the early portion of the explosion. At the same time the density in real air happens to be noticeably higher. All this points to the lower temperature at the front in real air. Above the heights of $8 \div 10$ km other effects due to the difference in atmosphere models are added. As to the lowering shock, as it was mentioned above, those effects are rather negligible.

Considering on the whole the influence of the real atmosphere non-isothermal properties and air high-temperature physical-chemical characteristics, one should note their contrary, to some extent, nature. A study of the real air properties at high temperatures leads to the largest difference in results reaching 100% at an early stage of the process. Then the difference gradually disappears. On the contrary, the standard atmosphere re-

sults deviate from those of the isothermal atmosphere more and more with the time and distance covered by the shock wave. At some instants in some regions there may occur conditions where one effect may compensate the other. From this point of view their separate consideration here is useful.

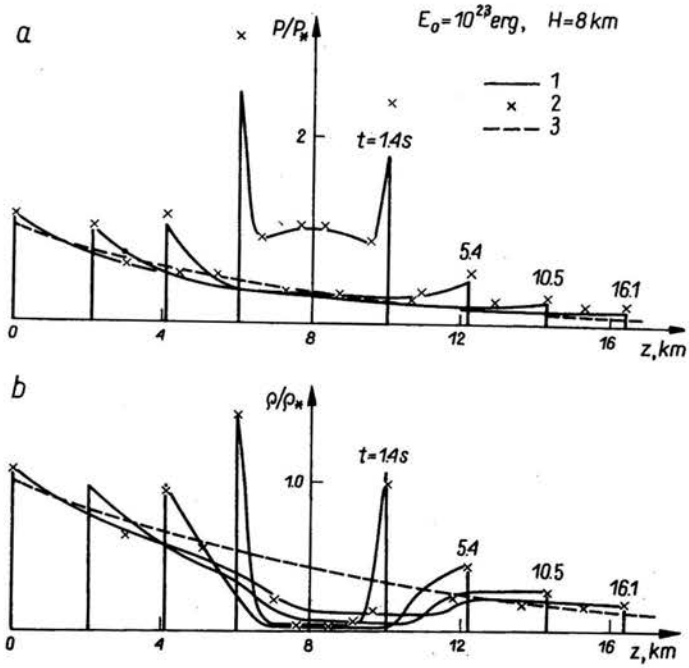

FIG. 6. Pressure and density distributions along the vertical at different times.
1 — real gas, standard atmosphere, 2 — perfect gas, exponential atmosphere 3 — undisturbed atmosphere pressure and density.

5. Tunguska meteorite problem

The results discussed above are of interest, in particular, for the gasdynamical simulation of a shock wave system arising during the flight and explosion-like disintegration of a cosmic body in the Earth's atmosphere and for the solution of the corresponding inverse problem. These questions in application to the Tunguska meteorite problem were dealt with in works [8–13] by V. P. KOROBEINIKOV, P. I. CHUSHKIN and L. V. SHURSHALOV. Some initial results of this investigation were reported at the 10th International Symposium on Modern Problems and Methods in Fluid and Gas Dynamics (Poland, 1971) [8]. In those works the mentioned shock waves system is simulated by a wave system arising from the explosion of a semi-infinite cylindrical charge with variable specific energy along its axis, the charge's axis being directed along the trajectory and its end point being located at the point of the atmosphere where the meteorite exploded. Since the inclination angle of the trajectory, the height of its final point (of explosion), the energetic parameters of the Tunguska explosion are not known beforehand, then an inverse problem arises: the basic parameters of the model explosion must be found so that the calculated consequences of the

blast be close to the observed ones. As it is known, the main and well studied result of the Tunguska explosion is the forest flattening in the catastrophy region. The forest destruction zone investigated in detail by FAST *et al.* [18–19] is shown in Fig. 7a. It has a number of peculiarities:

1) The outer boundary of the zone has a specific form resembling a butterfly.

2) The approximately radial character of the forest flattening appears in the main part of the zone.

3) Some systematic deviations from radial directions are observed near the edges of the "butterfly wings".

4) A small region (approximately 5 km in diameter) of standing dead trees without branches is present near the epicentrum of the explosion.

5) The areas of maximum destructions are situated approximately symmetrically at 1/3 of the distance from the epicentrum to the edges of the "butterfly wings".

The gasdynamical problem of the propagation in the Earth's atmosphere of shock waves arising from the explosion of a semi-infinite cylindrical charge with variable specific energy along its axis is a complicated one. An effective method combining two-dimensional computational and approximate numerical approaches was worked out in [8–12]. In this method both the reflection of shock waves from the ground and the non-homogeneity of the Earth's atmosphere are taken into consideration. The latter factor was initially calculated by means of the Sachs scaling rule, then an improved technique based on matching the Sachs rule with a well-known asymptotic solution for weak shock waves in a non-uniform medium was set up.

A large series of caculations carried out gave the theoretical picture of ground destructions shown in Fig. 7b. The outer boundary of the flattened forest zone is drawn by the solid curve corresponding to the value of dynamic pressure $q = \varrho u^2$ (u is the horizontal air velocity near the ground) equal to 0.008 kg/cm^2. About 5% of all the trees are thrown down by such a "wind". The directions of the fallen trees are plotted by the arrows. The dashed lines represent isochrones, i.e. the lines of shock waves reaching the ground at various times. Between the calculated (Fig. 7b) and the observed (Fig. 7a) pictures of the flattened forest, a good qualitative and quantitative correspondence exists in all the characteristic features mentioned above. The following basic trajectory and energetic parameters were found as a result of these calculations: the angle of the trajectory inclination to the Earth's surface $\alpha = 40°$, the height of the explosion at the final point of the trajectory $H = 6.5$ km, the specific energy of the ballistic wave $E_{0c} = 1.4 \cdot 10^{17}$ erg/cm, the energy of the final explosion $E_{0s} = 10^{23}$ erg. The combined energies of the blast and ballistic waves responsible for the forest flattening is equal to about 9.5 M ton. The total TNT equivalent to the Tunguska event may be approximately 1.5 times more than this figure if one takes into account all the factors put aside for the present. The latest estimates [20] of the Tunguska event TNT equivalent, obtained on the basis of available barograms and seismograms, are found to be 12.5 ± 2.5 M ton, in good correspondence with our results.

The question arises as to how accurate the solution of the inverse problem for the Tunguska meteorite is and whether it is single-valued. As to the accuracy, one should note that the obtained solution may be improved by taking into consideration a number of

additional factors such as real physical-chemical properties of air at high temperatures, radiation processes, the three-dimensional character of the real flow, more exact data concerning the flattened forest zone, etc. From this point of view the results presented above of shock wave calculations in the real atmosphere contribute to a better under-

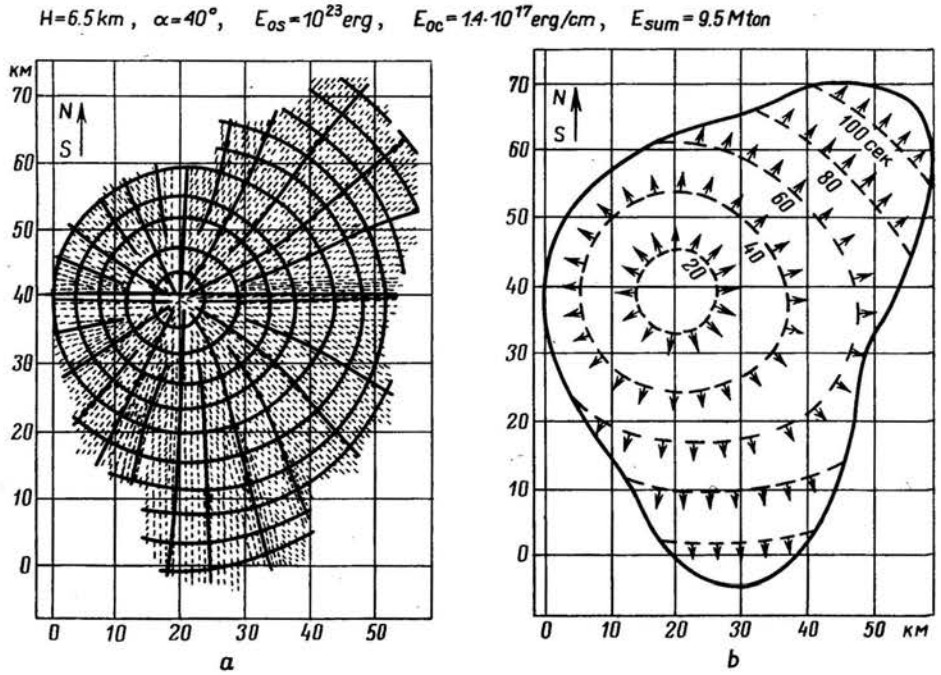

FIG. 7. Real and calculated pictures of the Tunguska forest flattening.

standing of the influence of various factors. When applied to the solution of the inverse problem these results will give more accuratly the trajectory and, especially, the energetic parameters of the Tunguska event.

As regards the uniqueness of the solution, it may not be unique theoretically. But the practice of calculations shows that the more complete information about the forest flattening zone is taken into account, the less probable becomes the same solution with some other combination of the basic parameters in the model considered. For example, the outer boundary of the flattened forest zone close to the real one may be obtained with various sets of parameters (in particular with $\alpha = 30°$) in the gasdynamical model [12]. But the combination of those parameters becomes practically unique if one considers not only the outer boundary but also the inner structure of the destruction zone. Thus the Tunguska meteorite trajectory and energetic parameters determined in [10, 12] are quite reliable within the limits of the model chosen and available information about the real forest flattening. It is quite another matter that some other models of the Tunguska event may be applied to the calculation of the forest destruction zone. But no one as yet has made such calculations by means of other models.

References

1. В. П. Карликов, *Решение линеаризованной осесимметричной задачи о точечном взрыве в среде с переменной плотностью*, Докл. АН СССР, **101**, 6, 1009–1012, 1955.
2. D. D. Laumbach, R. F. Probstein, *A point explosion in a cold exponential atmosphere*, J. Fluid Mech., **35**, Part I, 53–75, 1969.
3. Х. С. Кестенбойм, Ф. Д. Турецкая, Л. А. Чудов, *Точечный взрыв в неоднородной атмосфере*, Журнал прикл. мех. техн. физ., 5, 25–28, 1969.
4. Х. С. Кестенбойм, Г. С. Росляков, Л. А. Чудов, *Точечный взрыв. Методы расчета. Таблицы*, Изд. Наука, Москва 1974.
5. Л. В. Шуршалов, *О расчете ударных волн, распространяющихся в неоднородной атмосфере*, Докл. АН СССР, **230**, 4, 803–806, 1976.
6. С. К. Годунов, *Разностный метод численного расчета разрывных решений уравнений гидродинамики*, Мат. сборник, **47**, 3, 271–306, 1959.
7. С. К. Годунов, А. В. Забродин, Г. П. Прокопов, *Разностная схема для двумерных нестационарных задач газовой динамики и расчет обтекания с отошедшей волной*, Журнал вычис. мат. и матем. физ., **1**, 6, 1020–1050, 1961.
8. V. P. Korobeinikov, P. I. Chushkin, L. V. Shurshalov, *Gas dynamics of flight and explosion of meteorite bodies in the Earth's atmosphere*, Fluid Dyn. Trans. (ed. W. Fiszdon, Z. Płochocki, M. Bratos), **6**, Part II, 351–359, PWN, Warszawa 1971.
9. V. P. Korobeinikov, P. I. Chushkin, L. V. Shurshalov, *Gas dynamics of the flight and explosion of meteorites*, Astronautica Acta, **17**, 4/5, 339–348, 1972.
10. V. P. Korobeinikov, P. I. Chushkin, L. V. Shurshalov, *Mathematical model and computation of the Tunguska meteorite explosion*, Acta Astronautica, **3**, 7/8, 615–622, 1976.
11. В. П. Коробейников, П. И. Чушкин, Л. В. Шуршалов, *О зоне наземных разрушений при воздушном взрыве крупного метеорита*, Изв. АН СССР, Мех. жидкости и газа, 3, 94–100, 1974.
12. В. П. Коробейников, П. И. Чушкин, Л. В. Шуршалов, *О расчете наземных разрушений при воздушном взрыве метеорита*, Космическое вещество на Земле (Проблема Тунгусского метеорита), Изд. Наука, 54–65, Новосибирск 1976.
13. В. П. Коробейников, П. И. Чушкин, Л. В. Шуршалов, *Об учете неоднородности атмосферы при ресчете взрыва Тунгусского метеорита*, Журнал выч. мат. и матем. физ., **17**, 3. 737–752, 1977.
14. Н. М. Кузнецов, *Термодинамические функции и ударные адиабаты воздуха при высоких температурах*, Изд. Машиностроение, Москва 1965.
15. H. L. Brode, *Blast wave from a spherical charge*, Phys. Fluids, **2**, 2, 217–229, 1959.
16. B. S. Masson, T. D. Taylor, R. M. Foster, *Application of Godunov's method to blunt body calculation*, AIAA, **7**, 4, 694–698, 1969.
17. M. Lutzky, D. L. Lehto, *Shock propagation in spherically symmetric exponential atmospheres*, Phys. Fluids, **11**, 7, 1466–1472, 1968.
18. В. Г. Фаст, *Вывал леса, произведенный Тунгусским метеоритом*, Современное состояние проблемы Тунгусского метеорита, Вопросы метеоритики, Изд. Томского унив., 41–42, 1971.
19. В. Г. Фаст, А. П. Баранник, С. А. Разин, *О поле направлений повала деревьев в районе падения Тунгусского метеорита*, Вопросы метеоритики, Изд. Томского унив., 39–52, Томск 1976.
20. A. Ben-Menahen, *Source parameters of the Sibirian explosion of June 30, 1908, from analysis and synthesis of seismic signals at four stations*, Phys. Earth and Planetary Interiors, **11**, 1–35, 1975.

COMPUTING CENTRE OF THE USSR ACADEMY OF SCIENCES, MOSCOW, USSR.

Received September 27, 1977.